Current Biology 18, 1778–1784, November 25, 2008 ©2008 Elsevier Ltd All rights reserved DOI 10.1016/j.cub.2008.08.012

Report

# Kinetochore-Microtubule Attachment Relies on the Disordered N-Terminal Tail Domain of Hec1

**Geoffrey J. Guimaraes,[1] Yimin Dong,[2] Bruce F. McEwen,[2] and Jennifer G. DeLuca[1,*]**
[1]Department of Biochemistry and Molecular Biology
Colorado State University
Fort Collins, CO 80523-1870
USA
[2]Wadsworth Center
New York State Department of Health
Albany, NY 12201
USA

## Summary

**Accurate chromosome segregation is dependent upon stable attachment of kinetochores to spindle microtubules during mitosis. A long-standing question is how kinetochores maintain stable attachment to the plus ends of dynamic microtubules that are continually growing and shortening. The Ndc80 complex is essential for persistent end-on kinetochore-microtubule attachment in cells [1, 2], but how the Ndc80 complex forms functional microtubule-binding sites remains unknown. We show that the 80 amino acid N-terminal unstructured "tail" of Hec1 is required for generating stable kinetochore-microtubule attachments. PtK1 cells depleted of endogenous Hec1 and rescued with Hec1-GFP fusion proteins deleted of the entire N terminus or the disordered N-terminal 80 amino acid tail domain fail to generate stable kinetochore-microtubule attachments. Mutation of nine amino acids within the Hec1 tail to reduce its positive charge also abolishes stable attachment. Furthermore, the mitotic checkpoint remains functional after deletion of the N-terminal 80 amino acid tail, but not after deletion of the N-terminal 207 amino acid region containing both the tail domain and a calponin homology (CH) domain. These results demonstrate that kinetochore-microtubule binding is dependent on electrostatic interactions mediated through the disordered N-terminal 80 amino acid tail domain and mitotic-checkpoint function is dependent on the CH domain of Hec1.**

## Results and Discussion

We set out to determine the molecular requirements for kinetochore-microtubule attachment in vivo by utilizing a silence and rescue system for Hec1 in PtK1 cells. The PtK1 genome is not yet sequenced; thus, to deplete Hec1 with RNA interference (RNAi), we cloned PtK1 *HEC1* by using techniques described previously [3]. Consistent with its highly conserved role in chromosome segregation, PtK1 Hec1 is 71% identical to human Hec1 at the amino acid level (Figure S1A available online). Treatment of PtK1 cells with small interfering RNA (siRNA) targeted to *HEC1* for 48 hr resulted in a reduction of Hec1 in the cell population to approximately 50% of control as determined by western blotting (data not shown). This is probably reflective of poor transfection efficiency, given that cells positively transfected with fluorescently labeled Hec1 siRNA were depleted of kinetochore-bound Hec1 to an average of 8%, with many kinetochores from individual cells binding undetectable levels of Hec1, as determined by fluorescence-intensity measurements (Figures 1A and 1B).

Hec1-depleted PtK1 cells were able to form bipolar spindles, but they failed to align their chromosomes at the spindle equator (Figure 1B), consistent with findings in other cell types [1, 2]. We determined whether kinetochores were associated with the ends of spindle microtubules by analyzing deconvolved images of PtK1 cells fixed and immunostained for microtubules and kinetochores. On average, only 5% of kinetochores in Hec1-depleted cells contained end-on microtubule attachments, compared to 60% and 84% of kinetochores in early-to-mid-prometaphase and late-prometaphase control cells, respectively (Figure 1C). We measured the interkinetochore distance between sister kinetochores to determine whether they were under tension, and we found that, in contrast to mock-transfected cells, Hec1-depleted cells failed to establish tension across sister kinetochores during progression through mitosis (Figure 1D). Additionally, Hec1-depleted cells retained few microtubules after a cold-induced microtubule-depolymerization assay (Figure 1E). Together, these results demonstrate that Hec1 is required for stable kinetochore-microtubule attachment in PtK1 cells.

Time-lapse imaging demonstrated that Hec1-siRNA-transfected cells failed to align their chromosomes, but they did not arrest in mitosis and entered anaphase after a ~40 min delay when compared to mock-transfected cells (Figures 1F and 1G, Movies S1 and S2, and Figure S2). Hec1-depleted PtK1 cells failed to retain high levels of the spindle-checkpoint protein Mad2 at unattached kinetochores (Figure S3), consistent with findings in other cell types [4–8]. The decrease in kinetochore-bound Mad2 was not due to a defect in Mad2 recruitment, given that kinetochores in Hec1-depleted, nocodazole-treated PtK1 cells bound high levels of Mad2 and subsequently arrested in mitosis for approximately 5 hr, similar to mock-transfected cells treated with nocodazole (Figures S2 and S3 and Movies S3 and S4).

A portion of the N terminus of Hec1 folds into a calponin homology (CH) domain, which is a motif found in both actin and microtubule-binding proteins [9–11]. N-terminal to the CH domain is a highly basic 80 amino acid tail domain. Its structure is unknown because it was deleted for facilitating production of crystals for X-ray crystallographic studies [12, 13]. This is not surprising, given that it is predicted to be intrinsically disordered and has a low probability of maintaining a stably folded conformation [14] (Figure S1B). The remainder of Hec1 is also predicted to be largely intrinsically disordered, but its dimerization with Nuf2 results in a stably maintained coiled-coil domain [2, 14]. To determine the role of the N terminus of Hec1 in mitosis, we depleted PtK1 cells of endogenous Hec1 and carried out rescue experiments by expressing C-terminal GFP fusions of human Hec1 (full-length) and Hec1 deleted of both its CH domain and 80 amino acid tail (Δ1–207 Hec1-GFP). N-terminal GFP fusions were also generated for Hec1 full-length and deletion constructs, and their expression produced results similar to those of the corresponding C-terminal fusion

*Correspondence: jennifer.deluca@colostate.edu

proteins (Figure S4). Rescue experiments in which either full-length Hec1-GFP or Δ1–207 Hec1-GFP were expressed in PtK1 cells depleted of endogenous Hec1 demonstrate that Δ1–207 Hec1-GFP was able to localize to kinetochores identically to full-length Hec1-GFP (Figure 2A). However, cells rescued with Δ1–207 Hec1-GFP failed to align their chromosomes at the spindle equator, in contrast to cells rescued with full-length Hec1-GFP (Figure 2A). The Δ1–207 Hec1-GFP rescue resulted in a reduction of end-on kinetochore-microtubule attachments, given that only ~20% of kinetochores were associated with microtubule plus ends in these cells (Figure 2B). This is significantly lower than that in cells rescued with full-length Hec1-GFP, whose end-on attachments increased from ~60% in early-to-mid prometaphase to ~80% in late prometaphase (Figure 2B). In addition, we measured interkinetochore distances between sister kinetochores in Δ1–207 Hec1-GFP-rescued cells and found that these kinetochores exhibited reduced tension (Figure 2C). These results demonstrate that the N-terminal 207 amino acids of Hec1 are required for efficient formation of kinetochore microtubules in PtK1 cells.

We next tested the role of the disordered 80 amino acid tail of Hec1 in kinetochore-microtubule attachment by generating a Δ1–80 Hec1-GFP mutant. Previous in vitro studies have shown that removal of the 80 amino acid tail domain from Hec1 does not disrupt the structure of the CH domain [12, 13]. When expressed in PtK1 cells, Δ1–80 Hec1-GFP localized to kinetochores but was incapable of compensating for endogenous Hec1-depletion defects. Similar to cells rescued with Δ1–207 Hec1-GFP, cells rescued with Δ1–80 Hec1-GFP failed to align their chromosomes, exhibited a reduction in end-on kinetochore-microtubule attachments, and exhibited reduced tension across sister kinetochore pairs (Figures 2A–2C). Thus, deletion of the 80 amino acid disordered tail domain of Hec1 results in kinetochores that are unable to generate a sufficient number of stable microtubule attachments required for chromosome biorientation in cells.

To determine the effect of expression of the Hec1 N-terminal deletion mutants on mitotic progression, we imaged cells transfected with Cy5-labeled Hec1 siRNA and GFP-labeled Hec1 fusion proteins via time-lapse microscopy. As shown in Figure 2D, cells rescued with Δ1–207 Hec1-GFP or Δ1–80 Hec1-GFP were unable to align their chromosomes at the spindle equator (Movies S5 and S6), confirming our fixed-cell immunofluorescence data. In contrast, most of the cells rescued with full-length Hec1-GFP managed to align their chromosomes into a metaphase plate (13 of 15 cells) and enter anaphase with an average time of 44 ± 15 min from nuclear-envelope breakdown (NEBD) to anaphase onset (Figures 2D and 2E and Movie S7). Similar to cells transfected with Hec1 siRNA alone, most Δ1–207 Hec1-GFP-rescued cells were not able to sustain a mitotic arrest in the presence of unaligned chromosomes, and they entered anaphase after a ~45 min delay (NEBD to anaphase onset: 86 ± 36 min, n = 23 cells; Figure 2F). However, most of the cells rescued with Δ1–80 Hec1-GFP maintained a mitotic arrest for at least 3 hr (33 of 38 cells). These results suggest that the CH domain of Hec1, but not the 80 amino acid tail, is required to maintain a functional spindle-assembly checkpoint in the presence of unattached kinetochores in PtK1 cells.

Given the striking effect on kinetochore-microtubule attachment in cells rescued with Δ1–80 Hec1-GFP, we investigated the ultrastructure of these kinetochores by electron microscopy. As shown in Figure 3A, serial section images of kinetochores in mock-transfected cells often displayed a distinct outer plate with multiple microtubules bound. Depletion of Hec1 resulted in distinct outer plates with few microtubules bound (Figure 3B). Rescue with full-length Hec1-GFP restored microtubule binding (Figure 3C), whereas rescue with Δ1–80 Hec1-GFP did not (Figure 3D), confirming our light-microscopy data. Kinetochores in Hec1-depleted cells with no rescue or rescued with Δ1–80 Hec1-GFP rarely bound more than four microtubules (Figure 3E). The detection of corona material also indicated that these kinetochores were in a largely unbound state [15, 16] (Figures 3B and 3D). In contrast, all kinetochores in mock-transfected cells and full-length Hec1-GFP-rescued cells had many bound microtubules, with an average of more than 20 microtubules per kinetochore (Figure 3E).

Detection of an outer plate in Hec1-depleted PtK1 cells is somewhat surprising because Nuf2 depletion from HeLa cells, which causes a concomitant reduction in Hec1, results in loss of the outer-plate structure [17, 18]. Currently, it is not clear whether this is due to a difference in cell type or other factors. Furthermore, it is not possible from two-dimensional images of conventionally prepared specimens to know for certain that the outer plates in the unbound kinetochores of Hec1-depleted and Δ1–80 Hec1-GFP-rescued cells are structurally the same as in unbound kinetochores of control cells. This issue will have to be resolved by more extensive structural studies.

The positively charged tail domain of Hec1 is a substrate for Aurora B kinase phosphorylation in vitro, and nine target sites within this domain of human Hec1 of have been identified by mass spectrometry [13, 19]. Two recent in vitro studies have shown that inclusion of purified Aurora B kinase in microtubule-pelleting assays decreased the binding affinity of purified Ndc80 complexes for microtubules [13, 20]. In addition, overexpression of a Hec1 mutant in which six Aurora B target residues within the tail domain were mutated to prevent phosphorylation resulted in robust kinetochore-microtubule attachment, but defects in chromosome alignment and kinetochore-microtubule attachment-error correction were observed [19]. These studies have led to the hypothesis that phosphorylation of Hec1 by Aurora B kinase may prevent tight binding of microtubules to kinetochores to promote microtubule release in cells. This is consistent with findings that Aurora B promotes microtubule turnover and attachment-error correction in budding yeast and mammalian cells [21, 22]. We tested this hypothesis by expressing a mutant in which the nine identified target Aurora B phosphorylation serine (S) or threonine (T) residues within the Hec1 N terminus were mutated to aspartic acid (D) to mimic constitutive phosphorylation and reduce the overall positive charge of the tail domain (Figure S1A). Hec1-depleted cells rescued with 9D-Hec1-GFP were unable to align their chromosomes, exhibited a decrease in kinetochore-microtubule end-on attachments, and failed to generate wild-type tension across sister kinetochores (Figures 4A–4C). This is in contrast to cells rescued with either full-length Hec1-GFP or a mutant in which the nine phosphorylation target sites were mutated to alanine (9A-Hec1-GFP), in which robust kinetochore-microtubule attachments were observed (Figure 4A). Although cells rescued with 9A-Hec1-GFP were able to generate kinetochore-microtubule attachments, they often exhibited defects in chromosome alignment, consistent with a previous overexpression study using a Hec1 alanine (A) mutant [19]. These experiments suggest that the charge composition of the 80 amino acid tail domain of Hec1 is a critical determinant of kinetochore-microtubule attachment.

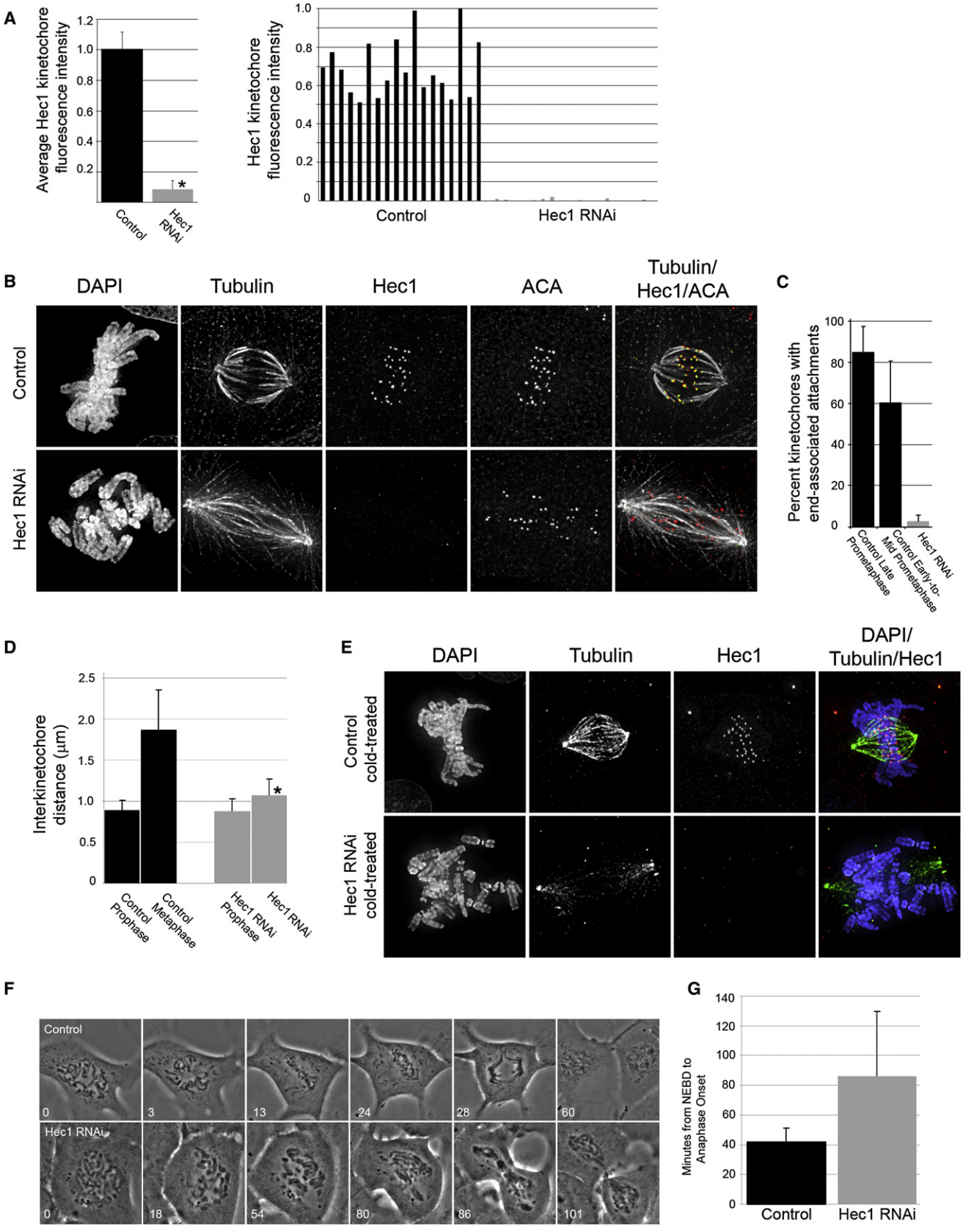


Figure 1. Hec1 Depletion from PtK1 Cells Results in Mitotic Defects

(A) Average Hec1 kinetochore fluorescence intensity in Hec1-siRNA-transfected and mock-transfected cells (left). Cells transfected with Cy5-labeled Hec1 siRNA were identified, and those with reduced levels of kinetochore-associated Hec1 were subjected to kinetochore fluorescence-intensity analysis (n = 11

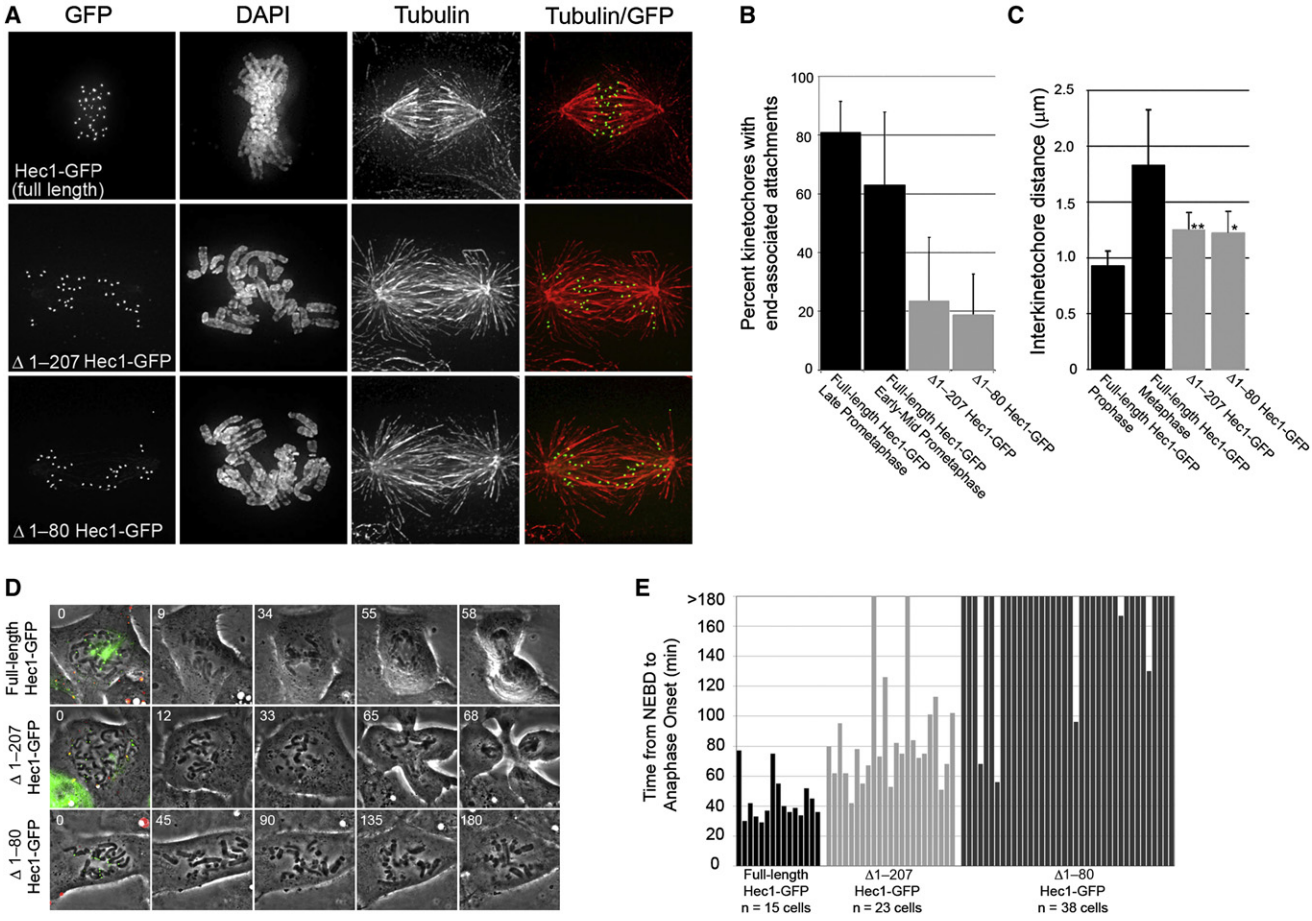


Figure 2. The N Terminus of Hec1 Is Required for Kinetochore-Microtubule Attachment

(A) Projections of deconvolved immunofluorescence images of PtK1 cells depleted of endogenous Hec1 and rescued with the indicated GFP fusion proteins.

(B) Quantification of end-on microtubule association with kinetochores (full-length Hec1-GFP, late prometaphase: n = 10 cells, 256 kinetochores; full-length Hec1-GFP, early-mid prometaphase: n = 10 cells, 251 kinetochores; Δ1–207 Hec1-GFP: n = 10 cells, 214 kinetochores; Δ1–80 Hec1-GFP: n = 10 cells, 217 kinetochores).

(C) Quantification of interkinetochore distances, which were measured from Hec1-GFP centroid to Hec1-GFP centroid (full-length Hec1-GFP, prophase: n = 11 cells, 46 kinetochore pairs; full-length Hec1-GFP, metaphase: n = 12 cells, 75 kinetochore pairs; Δ1–207 Hec1-GFP: n = 21 cells, 88 kinetochore pairs; Δ1–80 Hec1-GFP: n = 21 cells, 90 kinetochore pairs). The p values (indicated by the asterisk and double asterisk) are <0.0005, as measured by Student's t test (single asterisk: Δ1–80 Hec1-GFP versus full-length Hec1-GFP, metaphase; double asterisk: Δ1–207 Hec1-GFP versus full-length Hec1-GFP, metaphase).

(D) Image stills from time-lapse image acquisitions. Cells positive for both Cy5-labeled Hec1 siRNA and the GFP fusion protein indicated (first panel of each series) were identified and imaged with a 100× phase-contrast objective. Time is indicated in min.

(E) Quantification of mitotic timing (full-length Hec1-GFP: n = 15 cells; Δ1–207 Hec1-GFP: n = 23 cells; Δ1–80 Hec1-GFP: n = 38 cells). Time was scored from NEBD to anaphase onset. Cells were imaged for 3 hr, and those cells still in mitosis at the end of imaging were scored as >180 min. The vertical line in all bar graphs indicates the standard deviation.

---

cells, 170 kinetochores). Kinetochores from mock-transfected cells were also analyzed (n = 13 cells, 198 kinetochores), and the fluorescence was normalized to one. For one representative mock-transfected cell and one representative cell transfected with Cy5-labeled Hec1 siRNA, individual kinetochore intensities for all kinetochores within that cell are shown (right). The p value (indicated by the asterisk) is <0.0001, as measured by Student's t test.

(B) Images of mock-transfected and Hec1-siRNA-transfected cells. Cells were fixed 48 hr after transfection, immunostained with the indicated antibodies, imaged, and deconvolved. Projections of image stacks are shown. The overlay shows tubulin (white), anti-centromere antibodies (ACA; red), and Hec1 (green).

(C) Quantification of end-on microtubule association with kinetochores (mock-transfected, late prometaphase: n = 10 cells, 212 kinetochores; mock-transfected, early-mid prometaphase: n = 10 cells, 208 kinetochores; Hec1-siRNA-transfected: n = 10 cells, 229 kinetochores).

(D) Quantification of interkinetochore distances, which were measured from ACA centroid to ACA centroid (mock-transfected, prophase: n = 5 cells, 25 kinetochore pairs; mock-transfected, metaphase: n = 14 cells, 61 kinetochore pairs; Hec1-siRNA-transfected, prophase: n = 10 cells, 77 kinetochore pairs; Hec1-siRNA-transfected: n = 32 cells, 307 kinetochore pairs). The asterisk indicates a p value of <0.0005, as measured by Student's t test (Hec1-siRNA-transfected versus mock-transfected, metaphase).

(E) Mock-transfected and Hec1-siRNA-transfected cells were subjected to a cold-induced microtubule-depolymerization assay, processed for immunofluorescence, immunostained with the indicated antibodies, imaged, and deconvolved. Projections of image stacks are shown.

(F) Time-lapse image stills of mock-transfected and Hec1-siRNA-transfected cells. Elapsed time is indicated in min.

(G) Average time for progression through mitosis for mock-transfected (n = 28 cells) and Hec1-siRNA-transfected (n = 86 cells) PtK1 cells. Time was scored from nuclear-envelope breakdown (NEBD) to anaphase onset. The vertical line in all bar graphs indicates the standard deviation.

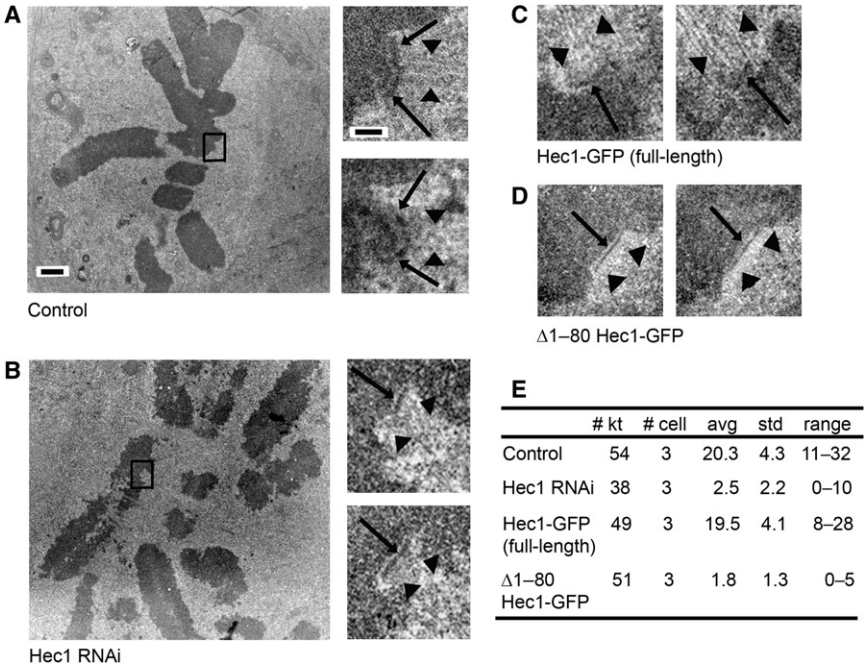


E

| | # kt | # cell | avg | std | range |
|---|---|---|---|---|---|
| Control | 54 | 3 | 20.3 | 4.3 | 11–32 |
| Hec1 RNAi | 38 | 3 | 2.5 | 2.2 | 0–10 |
| Hec1-GFP (full-length) | 49 | 3 | 19.5 | 4.1 | 8–28 |
| Δ1–80 Hec1-GFP | 51 | 3 | 1.8 | 1.3 | 0–5 |

Figure 3. Kinetochore Ultrastructure in Hec1-Depleted and Δ1–80 Hec1-GFP-Rescued PtK1 Cells

(A) Mock-transfected cell. On the left is a low-magnification image showing the metaphase alignment of the chromosomes. On the right are higher-magnification images of two serial sections through the kinetochore indicated by the box in the low-magnification view. Images show a distinct outer plate (indicated by arrows) and robust kinetochore fibers (indicated by arrowheads).

(B) Hec1-siRNA-transfected cell. On the left is a low-magnification image showing that Hec1 cells are unable to achieve metaphase alignment or form robust kinetochore fibers. On the right are higher-magnification images of two serial sections through the kinetochore indicated by the box in the low-magnification image. Although a distinct outer plate is frequently observed (indicated by arrows), few bound microtubules were detected. In addition, a fibrous corona characteristic of unbound kinetochores is evident (indicated by arrowheads). The scale bar for low-magnification images in (A) and (B) represents 1.0 μm.

(C) Hec1-depleted cells rescued with full-length Hec1-GFP. High-magnification views showing a distinct outer plate (indicated by arrows) with numerous bound microtubules (indiated by arrowheads), similar to that seen in (A).

(D) Hec1-depleted cells rescued with Δ1–80 Hec1-GFP. High-magnification views show unbound kinetochores with distinct outer plate (indicated by arrows) and corona (indicated by arrowheads), similar to that seen in (B). The scale bar for high-magnification images in (A)–(D) represents 200 nm.

(E) Quantification of kinetochore-microtubule attachment. The number of kinetochores scored (# kt), number of cells analyzed (# cell), average number of attached microtubules per kinetochore (avg), standard deviation (std), and range of attached microtubules per kinetochore (range) are listed for each experimental condition.

Both N termini of Hec1 and Nuf2 contain CH domains [12, 13], which have been implicated in microtubule binding [9, 11]. We show here that the 80 amino acid unstructured tail domain of Hec1 is required for the efficient formation of stable kinetochore-microtubule attachments in cells, and the CH domains of Hec1 and Nuf2 are not sufficient to carry out this task alone. Our findings are corroborated by recent in vitro data that demonstrate a decrease in binding affinity of the Ndc80 complex for microtubules upon deletion of the 80 amino acid Hec1 tail domain [12, 13]. It is surprising, however, that in the context of a living cell, defects due to deletion of this domain are not rescued by either redundant microtubule-binding factors at kinetochores or by the CH domains in Hec1 and Nuf2 themselves [13, 20].

What is the role of the 80 amino acid tail domain at the kinetochore-microtubule interface? Our results suggest that the tail domain mediates kinetochore-microtubule binding through electrostatic interactions. Nine amino acid substitutions within the Hec1 tail domain were made to mimic the charge brought on by phosphorylation. When these nine target residues within the tail domain were mutated to aspartic acid (D), the isoelectric point of this domain decreased from ~10.8 to ~8.0, and we observed a kinetochore-null phenotype, in which chromosomes failed to align and very few stable end-on kinetochore-microtubule attachments were generated. Loss of kinetochore-microtubule attachments due to a change in the charge composition of the Hec1 tail domain has important implications for how the cell generates and regulates kinetochore-microtubule attachments. Microtubules extend from their surface highly acidic C-terminal tail domains of alpha and beta tubulin. These tail domains can be cleaved by subtilisin, which reduces the affinity of a truncated, engineered Ndc80 complex ($Ndc80^{bonsai}$) for microtubules in vitro [13]. A model for kinetochore-microtubule attachment can be envisioned in which the N-terminal tail domains of Hec1 bind directly to the C-terminal acidic domains of tubulin and charge modification of Hec1 tails through phosphorylation regulates attachment status.

In support of this model, the tail domain of Hec1 is a substrate for Aurora B kinase in vitro [13, 19, 20]. Mutation of multiple residues in the tail domain to prevent phosphorylation in vivo results in robust kinetochore-microtubule attachment, whereas mutation of these residues to mimic constitutive phosphorylation in vivo results in loss of kinetochore-microtubule attachment (Figure 4). It is likely that mutation of multiple phosphorylation sites is required for an effect on kinetochore-microtubule attachment, and a single site may not modify the charge to a level that will induce detachment. Aurora B kinase phosphorylates *C. elegans* Ndc80 in vitro, and mutation of four consensus Aurora B kinase phosphorylation sites to alanine (probably corresponding to residues 5, 15, 44, and 55 in human Hec1) prevents phosphorylation [20], suggesting that one or more of these four residues is a key phosphorylation target. Future work is needed to test the minimum number of Hec1 point mutations that are required to elicit an attachment phenotype in vertebrate cells and to determine which specific residues or combinations of residues are the effectors of the phenotype. Our data support a model in which the tail domain of Hec1 acts as a regulator of kinetochore-microtubule attachment in cells. When kinase activity is elevated, the tail domain is phosphorylated, and microtubule turnover at the kinetochore-microtubule interface is high. As chromosomes align at the spindle equator, kinase activity decreases at the outer kinetochore, the tail domain of Hec1 becomes dephosphorylated, and kinetochore-microtubule attachments are stabilized. Future studies that correlate Hec1 phosphorylation in vivo with chromosome biorientation status will be key in testing this model.

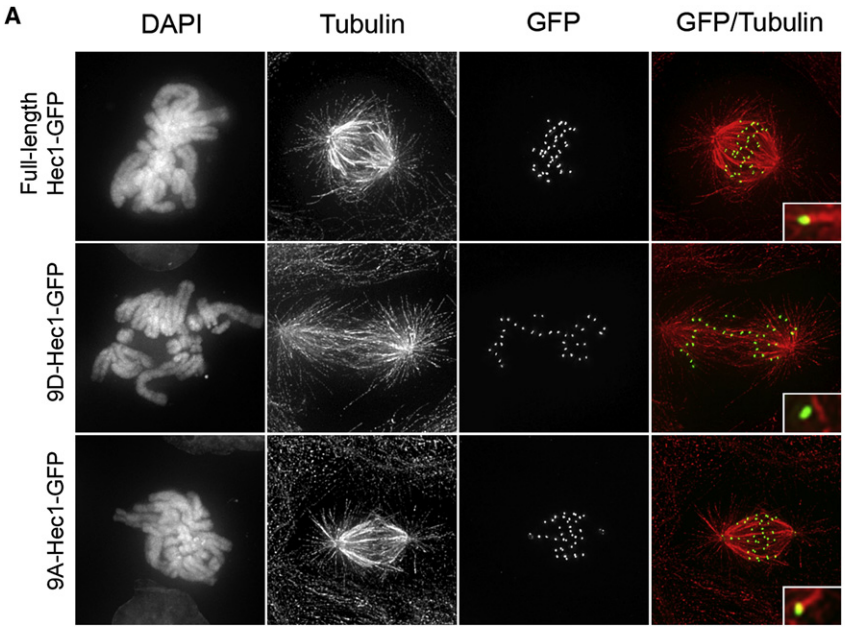


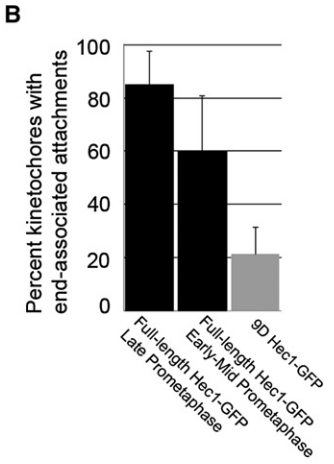


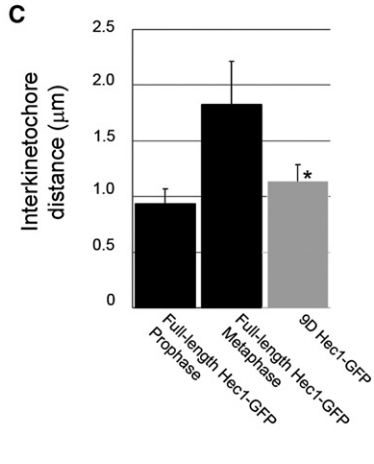


Figure 4. Charge Modification of the Hec1 80 Amino Acid Tail Domain Inhibits Kinetochore-Microtubule Attachment

(A) Deconvolved immunofluorescence images of Hec1-depleted PtK1 cells expressing the indicated GFP fusion proteins. The insets show higher-magnification images of individual kinetochores.

(B) Quantification of end-on microtubule association with kinetochores. Full-length Hec1-GFP data from Figure 2 are compared to data from 9D-Hec1-GFP-expressing cells: n = 10 cells, 295 kinetochores.

(C) Quantification of interkinetochore distances, measured from Hec1-GFP centroid to Hec1-GFP centroid (full-length Hec1-GFP, metaphase data from Figure 2 are compared to data from 9D-Hec1-GFP: n = 10 cells, 82 kinetochore pairs). The p value (indicated by asterisk) is <0.0005, as measured by Student's t test (9D-Hec1-GFP versus full-length Hec1-GFP, metaphase). The vertical line in all bar graphs indicates the standard deviation.

Our findings do not rule out recently proposed alternative models in which the N-terminal tail domain of Hec1 mediates kinetochore-microtubule binding by tethering Ndc80 complexes together at the kinetochore-microtubule interface [13]. Here, direct binding of the Ndc80 complexes to microtubules is largely mediated by electrostatic interactions between positive residues within the CH domains of Nuf2 and Hec1 and the C-terminal tubulin tails. In support of this model, the affinity of the Ndc80$^{bonsai}$ complex for microtubules was significantly reduced when point mutations were made in the CH domain of either Nuf2 or Hec1 that reduced the positive charge of these domains [13].

Although the 80 amino acid N-terminal tail domain is required for kinetochore-microtubule attachment, it is not needed to maintain the mitotic checkpoint. The CH domain, however, is required. A previous study has demonstrated an interaction between Hec1 and the Mad2-binding partner Mad1 in a yeast two-hybrid assay [4]. It will be important to establish whether the CH domain of Hec1 directly mediates this binding to Mad1 or to other mitotic-checkpoint factors. It will also be important to determine whether loss of the Hec1 CH domain affects the ability of Nuf2 to participate in checkpoint protein binding.

### Supplemental Data

Supplemental Data include Supplemental Experimental Procedures, four figures, and seven movies and can be found with this article online at http://www.current-biology.com/supplemental/S0960-9822(08)01052-X.

### Acknowledgments

We thank Alexey Khodjakov for PA-GFPTub-PtK1 cells, Ted Salmon for Mad2 antibodies, and Walt Gall and Ted Salmon for the parent GFP-9D-Hec1 construct. We thank Claire Walczak and Jane Stout for advice regarding PtK1 RNAi. Initial reagents to begin this work were generated in the Salmon lab (NIHGM24364 to Ted Salmon). We thank Keith DeLuca for technical help and critical reading of the manuscript. The authors thank Chad Pearson and O'Neil Wiggan for providing insightful comments on the manuscript. This work was supported by National Institutes of Health grants K01CA125051 to J.G.D. and RO1GM06627 to B.F.M. and by a Basil O'Conner Starter Scholar Research Award to J.G.D.

Received: June 26, 2008
Revised: August 4, 2008
Accepted: August 7, 2008
Published online: November 20, 2008

### References

1. Maiato, H., DeLuca, J., Salmon, E.D., and Earnshaw, W.C. (2004). The dynamic kinetochore-microtubule interface. J. Cell Sci. *117*, 5461–5477.
2. Cheeseman, I.M., and Desai, A. (2008). Molecular architecture of the kinetochore- microtubule interface. Nat. Rev. Mol. Cell Biol. *9*, 33–46.
3. Stout, J.R., Rizk, R.S., Kline, S.L., and Walczak, C.E. (2006). Deciphering protein function during mitosis in PtK cells using RNAi. BMC Cell Biol. *7*, 26–41.
4. Martin-Lluesma, S., Stucke, V.M., and Nigg, E.A. (2002). Role of Hec1 in spindle checkpoint signaling and kinetochore recruitment of Mad1/Mad2. Science *297*, 2267–2270.
5. Hori, T., Haraguchi, T., Hiraoka, Y., Kimura, H., and Fukagawa, T. (2003). Dynamic behavior of Nuf2-Hec1 complex that localizes to the

centrosome and centromere and is essential for mitotic progression in vertebrate cells. J. Cell Sci. *116*, 3347–3362.

6. DeLuca, J.G., Howell, B.J., Canman, J.C., Hickey, J.M., Fang, G., and Salmon, E.D. (2003). Nuf2 and Hec1 are required for retention of the checkpoint proteins Mad1 and Mad2 to kinetochores. Curr. Biol. *13*, 2103–2109.
7. Bharadwaj, R., Qi, W., and Yu, H. (2004). Identification of two novel components of the human NDC80 kinetochore complex. J. Biol. Chem. *279*, 13076–13085.
8. Meraldi, P., Draviam, V.M., and Sorger, P.K. (2004). Timing and checkpoints in the regulation of mitotic progression. Dev. Cell *7*, 45–60.
9. Gimona, M., Djinovic-Carugo, K., Kranewitter, W.J., and Winder, S.J. (2002). Functional plasticity of CH domains. FEBS Lett. *513*, 98–106.
10. Slep, K.C., and Vale, R.D. (2007). Structural basis of microtubule plus end tracking by XMAP215, CLIP-170, and EB1. Mol. Cell *27*, 976–991.
11. Korenbaum, E., and Rivero, F. (2002). Calponin homology domains at a glance. J. Cell Sci. *115*, 3543–3545.
12. Wei, R.R., Al-Bassam, J., and Harrison, S.C. (2007). The Ndc80/HEC1 complex is a contact point for kinetochore-microtubule attachment. Nat. Struct. Mol. Biol. *14*, 54–59.
13. Ciferri, C., Pasqualato, S., Screpanti, E., Varetti, G., Santaguida, S., Dos Reis, G., Maiolica, A., Polka, J., De Luca, J.G., De Wulf, P., et al. (2008). Implications for kinetochore- microtubule attachment from the structure of an engineered Ndc80 complex. Cell *133*, 427–439.
14. Prilusky, J., Felder, C.E., Zeev-Ben-Mordehai, T., Rydberg, E.H., Man, O., Beckmann, J.S., Silman, I., and Sussman, J.L. (2005). FoldIndex: A simple tool to predict whether a given protein sequence is intrinsically unfolded. Bioinformatics *21*, 3435–3438.
15. Cassimeris, L., Rieder, C.L., Rupp, G., and Salmon, E.D. (1990). Stability of microtubule attachment to metaphase kinetochores in PtK1 cells. J. Cell Sci. *96*, 9–15.
16. Howell, B.J., McEwen, B.F., Canman, J.C., Hoffman, D.B., Farrar, E.M., Rieder, C.L., and Salmon, E.D. (2001). Cytoplasmic dynein/dynactin drives kinetochore protein transport to the spindle poles and has a role in mitotic spindle checkpoint inactivation. J. Cell Biol. *155*, 1159–1172.
17. DeLuca, J.G., Dong, Y., Hergert, P., Strauss, J., Hickey, J.M., Salmon, E.D., and McEwen, B.F. (2005). Hec1 and Nuf2 are core components of the kinetochore outer plate essential for organizing microtubule attachment sites. Mol. Biol. Cell *16*, 519–531.
18. Liu, S.T., Rattner, J.B., Jablonski, S.A., and Yen, T.J. (2006). Mapping the assembly pathways that specify formation of the trilaminar kinetochore plates in human cells. J. Cell Biol. *175*, 41–53.
19. DeLuca, J.G., Gall, W.E., Ciferri, C., Cimini, D., Musacchio, A., and Salmon, E.D. (2006). Kinetochore microtubule dynamics and attachment stability are regulated by Hec1. Cell *127*, 969–982.
20. Cheeseman, I.M., Chappie, J.S., Wilson-Kubalek, E.M., and Desai, A. (2006). The conserved KMN network constitutes the core microtubule-binding site of the kinetochore. Cell *127*, 983–997.
21. Pinsky, B.A., Kung, C., Shokat, K.M., and Biggins, S. (2006). The Ipl1-Aurora protein kinase activates the spindle checkpoint by creating unattached kinetochores. Nat. Cell Biol. *8*, 78–83.
22. Cimini, D., Wan, X., Hirel, C.B., and Salmon, E.D. (2006). Aurora kinase promotes turnover of kinetochore microtubules to reduce chromosome segregation errors. Curr. Biol. *16*, 1711–1718.